Nancy McGuire in Noteworthy Chemistry (ACS) Winter 2015

http://www.acs.org/content/acs/en/noteworthy-chemistry/2015-archive/march-30.html#nc4

March 30, 2015

The fire is over, but the fire retardants linger on. Legal and regulatory restrictions have been successful in reducing the use of polybrominated diphenyl ether (PBDE) flame retardants, polychlorinated biphenyls (PCBs), and organochlorine pesticides (OCPs). These compounds, however, degrade very slowly in the environment, and older products manufactured from these compounds remain in use. PCBs and some PBDEs have been associated with various disruptions in human and animal physiological processes. Combustion products of PBDEs, including dioxins and furans, may be more toxic than the parent compounds.

J.-S. Park, R. W. Voss, and coauthors at the California Environmental Protection Agency (Berkeley), the California Department of Public Health (Richmond), the Sequoia Foundation (La Jolla, CA), and the University of California, Irvine, examined serum concentrations of PBDEs, PCBs, and OCPs for 101 southern California firefighters as part of the California Environmental Contaminant Biomonitoring Program. They collected detailed information about the participants' physiology, firefighting history, and gear maintenance and storage practices. They compared their results to those from other occupationally exposed groups (e.g., waste workers and foam-factory workers) and to less-exposed populations.

Firefighters exhibited high serum levels of PBDEs, in contrast to declining levels for Californians overall. Firefighters' levels of PCBs and OCPs were in line with nationwide levels. Multivariate analysis indicated that firefighters could reduce their serum levels of PCBs and OCPs (but not PBDEs) by having their turnout gear (trousers, jackets, boots, and helmets) professionally decontaminated after a fire.

The levels of some BDEs could be lowered by storing turnout gear in an open room rather than in enclosed lockers and by cleaning gear at the fire station rather than at the response site. Other factors included the use of self-contained breathing apparatuses during firefighting activities (regardless of whether the fire was inside or outside a structure) and the age of the fire station. (*Environ. Sci. Technol.* DOI: 10.1021/es5055918; Nancy McGuire)

http://www.acs.org/content/acs/en/noteworthy-chemistry/2015-archive/march-16.html#nc3

March 16, 2015

Are adrenaline and noradrenaline protectors or targets? The answer is "both", according to R. Álvarez-Diduk and A. Galano* of the Metropolitan Autonomous University–Iztapalapa (Mexico City). They used density functional theory calculations to investigate the roles of these catecholamine neurotransmitters (also known as epinephrine and norepinephrine) in organisms under oxidative stress, a condition associated with numerous human health and development disorders.

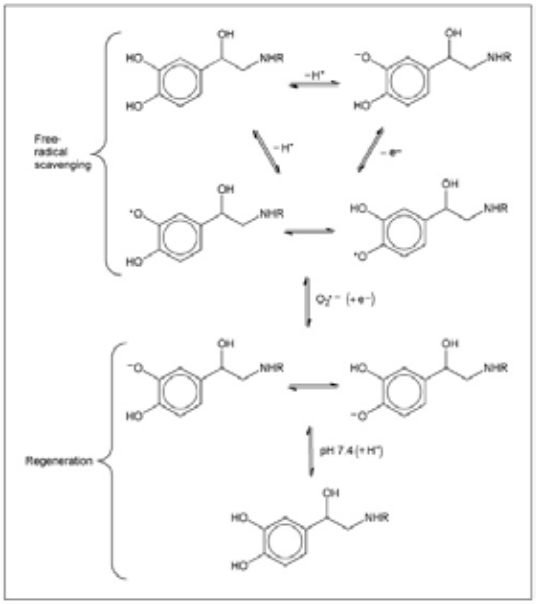

Mechanism of free-radical–scavenging activity and regeneration of adrenaline and noradrenaline

Adrenaline's role as a radical scavenger and metal chelator makes it an efficient antioxidant. Noradrenaline has been reported to provide short-term protection against β-amyloid–induced neurotoxicity associated with Alzheimer's disease; it also reduces the amounts of reactive oxygen species within cells, which might be useful for treating Parkinson's disease. Accumulations of the reaction products in the body, however, could pose a health risk.

The computational study predicts that adrenaline and noradrenaline can be efficient free-radical scavengers in lipids and aqueous media. The two compounds react with peroxyl radicals (•OOH) faster than the reference compound trolox (a water-soluble analogue of vitamin E), but they only partially inhibit oxidative stress induced by hydroxyl radicals (•OH) produced by the copper-catalyzed reaction of hydrogen peroxide with oxygen radicals ($O_2^{\bullet -}$). Their ability to sequester copper(II) ions by forming chelation complexes makes them efficient against Cu(II)–ascorbate mixtures.

The figure shows the mechanism of the free-radical–scavenging activity and regeneration of adrenaline (1, R = Me) and noradrenaline (1, R = H).

Under highly oxidative conditions, both compounds may lose their functionality as a result of their antioxidant activities, making them molecular targets. Under physiological conditions, both can be regenerated spontaneously and resume their activity unless the intermediates are consumed in reactions with other species.

Cyclic 3-hydroxymelatonin, a melatonin metabolite, forms particularly strong complexes with Cu(II), which may allow it to remove copper from adrenaline and noradrenaline complexes and allow the two catecholamines to resume their antioxidant activities. (*J. Phys. Chem. B* DOI: 10.1021/acs.jpcb.5b00052; Nancy McGuire)

http://www.acs.org/content/acs/en/noteworthy-chemistry/2015-archive/march-9.html#nc5

March 9, 2015

Convert a biomass component to value-added hydrocarbons in one step. Lignocellulosic biomass is an abundant, inexpensive chemical feedstock that does not compete with food supplies. Pentanediols derived from this biomass have been evaluated as potential monomers for polyesters and polyurethanes, but they could also help to replace petroleum compounds as a source of transportation fuels.

Previous attempts to generate benzene, toluene, ethylbenzene, and xylenes (BTEX) from biomass gave high yields of CO, CO2, coke, and other unwanted byproducts. Other attempts to convert biologically derived gases to liquefied petroleum gas (LPG; hydrocarbons in the C2–C5 range) were energy-intensive and produced unwanted polynuclear aromatics and oxygenates.

J. Lauterbach and coauthors at the University of South Carolina (Columbia) and the University of Delaware (Newark) deoxygenated pentanediols by using zeolite HZSM-5 as a solid acid catalyst. At temperatures between 325 and 450 °C at atmospheric pressure, they produced LPG and BTEX, obtaining as much as 94% carbon yield. Over a 40-h production run, they sustained a 91.5% carbon yield of the desired products, with a relatively steady product distribution. (There was a gradual shift away from paraffin products toward olefins and xylenes.) They observed minimal production of CO, CO_2, and coke; and they were able to regenerate the HZSM-5 catalyst multiple times.

The researchers passed a mixture of helium and vaporized 1,5-pentanediol or 1,2-pentanediol through a fixed-bed quartz reactor that contained the catalyst. They cooled the effluent gas to condense the less-volatile products, mostly toluene and xylenes with lesser amounts of benzene, ethylbenzene, and C9+ aromatics. Higher reaction temperatures shifted selectivity toward smaller hydrocarbon products. No oxygenated compounds were found in the organic liquid phase.

Water in the production stream did not severely degrade the catalyst. In fact, feeding water along with the pentanediol reduced coke formation and produced a higher carbon yield of BTEX and LPG, especially C2–C4 olefins. Water reduced the interaction between the pentanediol and the catalyst acid sites and contributed to the partial gasification of carbon deposits. The aqueous effluent was >99 wt% water. No unreacted pentanediol was detected. (*ACS Sustainable Chem. Eng.* DOI: 10.1021/sc500815c; Nancy McGuire)

http://www.acs.org/content/acs/en/noteworthy-chemistry/2015-archive/march-2.html#nc2

March 2, 2015

Dead-end pores can pump out trapped particles. Natural structures often contain "dead-end" pores, through which fluids cannot flow when conventional pressure-driven mechanisms are used. Pumping water into reservoirs, however, helps recover oil in dead-end geological channels; and biomolecules diffuse through muscle tissue in part through transport in dead-end pores.

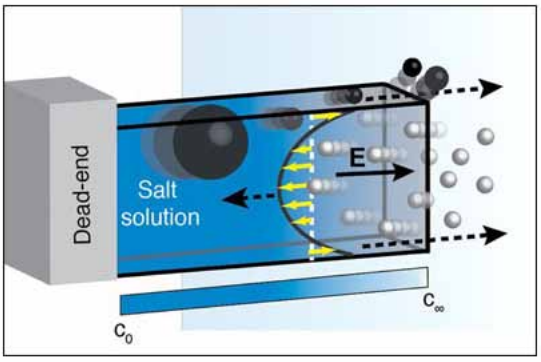

Schematic of diffusio-osmotic flow in a dead-end pore

A. Sen, D. Vegelol, and co-workers at Pennsylvania State University (University Park) show that particles and solutions can flow into and out of dead-end pores with the use of chemically driven convective flow and a phenomenon they call "transient diffusio-osmosis" (see schematic). The flow velocity depends on a transient electrolyte gradient, generated in situ, and the intrinsic charge on the pore wall.

The authors used glass capillary tubes to model dead-end pores. They prepared sodium chloride solutions with concentration gradients that varied with time; the gradients arose from the diffusion and convection of ionic species. To help visualize the flow patterns, they used two types of polystyrene latex beads: red 4-μm sulfate-functionalized beads and green 2-μm amine-functionalized beads.

The saline gradient in the solution generated an electric field, producing an electro-osmotic fluid flow near the pore wall. At the same time, the tracer beads migrated electrophoretically, independent of the electro-osmotic flow. The net observed transport rate was a combination of the two effects.

Video microscopy showed that the beads moved faster, and convective flow dominated over diffusion, near the mouth of the dead-end capillary. The amine-functionalized beads moved mostly by electro-osmosis; and their electrophoretic migration was slower than that of the sulfate-functionalized beads. The sulfate-functionalized beads moved toward the dead end, and the amine-functionalized beads moved toward the center of the capillary.

Carbonate solutions produced effects similar to the NaCl solutions. Beads in a potassium chloride gradient showed very little lateral motion, in contrast to the NaCl gradient, because potassium and chloride ions have almost identical diffusion coefficients and produce almost no electrical field. (*ACS Nano* DOI: 10.1021/nn506216b; Nancy McGuire)

http://www.acs.org/content/acs/en/noteworthy-chemistry/2015-archive/february-23.html#nc5

February 23, 2015

Cicada wings provide a clue to light harvesting. Cicada wings exhibit <1% light reflectance over the visible spectrum, which makes them very efficient at absorbing light. Design development for effective, economical light-harvesting structures is a new field; the cicada's light-harvesting ability would be useful for controlling the optical performance of these optoelectronic devices.

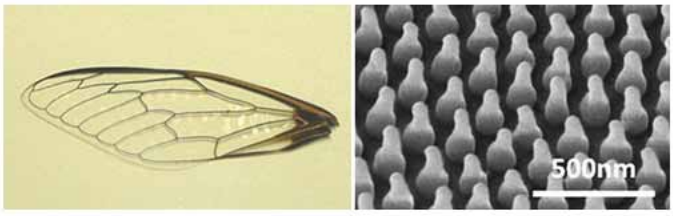

Photograph and scanning electron micrograph of a cicada wing

Cicada wing surfaces are covered in nanotip structures that resemble arrays of pointed spikes. The figure shows a photographic image (left) and a top-view scanning electron microscope image (right) of a cicada wing.

K.-H. Chen, S Chattopadhyay, and colleagues at National Yang Ming University, National Taipei University of Technology, National Taiwan University, and Academia Sinica (all in Taipei, Taiwan) created surface structures that imitate these spiky arrays by using low–refractive index (e.g., silica and indium tin oxide) and high-index (e.g., silicon and germanium) photovoltaic materials. The biomimetic structures had short spikes on the surface, whereas other structures had taller, sharper spikes. The authors varied the spacings, lengths, and refractive indices of the spikes to see which configurations came closest to the target of 1% reflectance or less.

The authors screened potential materials and geometries with the use of calculations and theoretical modeling. For silica, reflectance decreases almost to 1% as the ratio of the spike spacing to the incident light wavelength increases to almost 0.1. Greater spacing would be required to reduce the reflectance to the same degree for a material with a greater refractive index. Increasing the ratio of the spike lengths to their spacing also decreases reflectance.

The authors studied variations in the reflectance of laboratory samples with the angle of incidence and degree of polarization of the incident light. They found that, in contrast to a polished silicon surface, a silicon nanotip spike surface is remarkably insensitive to both of these factors at incident angles <70°; and it becomes even less sensitive as the length of the spikes increases. (*ACS Nano* DOI: 10.1021/nn506401h; Nancy McGuire)

http://www.acs.org/content/acs/en/noteworthy-chemistry/2015-archive/february-16.html#nc1

February 16, 2015

Bioinspired gels convert nitrogen to ammonia. Soybeans do it, peanuts do it, even educated cowpeas do it—they convert atmospheric nitrogen to ammonia in the soil, in the dark. The chemical industry does it faster, but the Haber–Bosch process requires an iron catalyst, high (≈400 °C) temperature, and high (≈250 bar) pressure. Making ≈200 million t of ammonia annually consumes >1% of the world's energy supply, according to M. G. Kanatzidis and co-workers at Northwestern University (Evanston, IL).

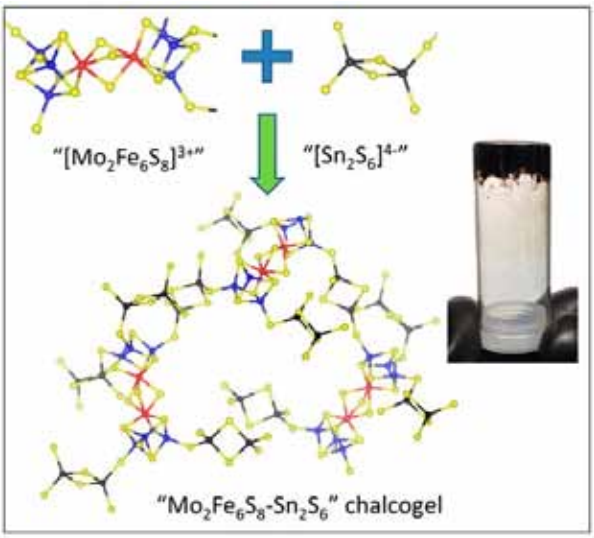

$Mo_2Fe_6S_8$–Sn_2S_6 chalcogel formation and structure (left); black chalcogel (right)

Nitrogen-fixing plants use nitrogenase enzymes that bind elemental nitrogen at iron molybdenum sulfide (FeMoS) core clusters. Nearby Fe–S clusters provide electrons that reduce the nitrogen to ammonia. The Northwestern group developed an accelerated version of the natural process by using FeMoS clusters and white light (or sunlight). They synthesized "chalcogels": black, spongy, porous gels composed of inorganic $Mo_2Fe_6S_8$ clusters linked by Sn_2S_6 ligands to form random, amorphous networks (see figure).

FeMoS catalysts previously were used to reduce hydrazine or hydrogen cyanide to ammonia, but they were ineffective at reducing elemental nitrogen except under strongly reducing conditions with electrochemical methods. Photochemical ammonia production without a catalyst requires ultraviolet light, semiconductor thin films, inert atmospheres, and temperatures as low as –78 °C.

In this study, the authors combined catalysis with photochemistry to produce ammonia from nitrogen with visible light, at room temperature, and under ambient pressure. They bubbled nitrogen through an aqueous solution of pyridinium hydrochloride (a proton source) and sodium ascorbate (an electron source) in which pieces of the chalcogel were immersed. The solutions were photolyzed with a 150-W xenon lamp. Isotope labeling tests confirmed that nitrogen gas was the source of the product ammonia.

Ammonia production began almost immediately and increased steadily over the 32-h test period. In a separate 72-h test, the researchers generated ≈8 equiv ammonia for each equivalent of catalyst, with no catalyst degradation or loss of activity. The chalcogel and light, proton, and electron sources are all necessary to make this method work. (*J. Am. Chem. Soc.* DOI: 10.1021/ja512491v; Nancy McGuire)

http://www.acs.org/content/acs/en/noteworthy-chemistry/2015-archive/february-9.html#nc4

February 9, 2015

The cigarette's the star in this movie. Solid-fuel combustion is a complex, poorly understood process at the microscopic level because it is difficult to obtain reproducible results. Fuel components dehydrate, release volatile compounds, ignite, and char at different rates. Multiple transient combustion and pyrolysis processes occur simultaneously, making them difficult to observe. These difficulties hamper studies of biomass and solid fossil fuel combustion.

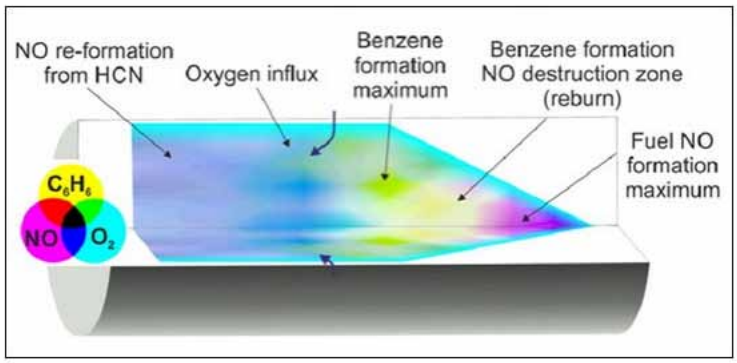

Depiction of burning cigarette

R. Zimmermann and coauthors at the University of Rostock, Helmholtz Center Munich (Neuherberg), and Photonion GmbH (Schwerin, all in Germany); and British American Tobacco (Southampton, UK) developed a method for observing and tracking solid-fuel combustion processes. They used standardized research cigarettes as a model biomass fuel. Cigarette-smoking machines and standard protocols, developed to study the health effects of smoking, were adapted to provide a uniform, reproducible combustion environment with uniform cycles of puffing and smoldering.

The researchers detected molecular ions of the combustion and pyrolysis products in real time by using a microprobe coupled to a photoionization mass spectrometer with soft laser single photon ionization. They repeated measurements in several locations along the cigarette to produce quantitative distribution maps of nitric oxide (NO), benzene, and oxygen, which they correlated with temperature profiles and flow vector maps.

The high temporal and spatial resolution of the resulting map sequences produced useful kinetic data as well as movie-like depictions of the formation and destruction of various compounds as the cigarette burned (see figure). (*Anal. Chem.* DOI: 10.1021/ac503512a; Nancy McGuire)

http://www.acs.org/content/acs/en/noteworthy-chemistry/2015-archive/february-2.html#nc3

February 2, 2015

Fano resonances make structural colors in thin films tunable. The iridescent "structural colors" in beetle shells, butterfly wings, and bird feathers are interference effects produced when light interacts with nanoscale structural features. Structural colors appear brighter in sunlight, do not bleach under prolonged exposure to light, and sometimes change when they are viewed at different angles.

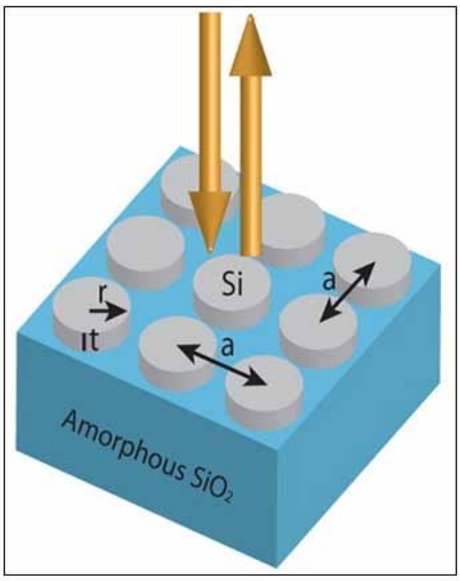

Silicon rods on a glass wafer

Structural color generation generally requires choosing between structures that are thick compared to the wavelength of the light or colors that cannot be tuned dynamically. Y. Shen and coauthors at MIT (Cambridge, MA) and Johannes Kepler University (Linz, Austria) found a way to combine tunability and thin films. They prepared thin photonic crystal slabs with resonance-induced colors that stayed almost the same at all viewing angles. They tuned the colors by stretching the slabs on an elastic substrate.

The authors describe a mechanism that produces color from interference between directly reflected light and the guided resonances mode on a surface structure. This mechanism is related to Fano resonance, in which light enters a periodic surface structure and excites a one-dimensionally confined mode supported by the surface structure. This localized mode "leaks" into the surrounding environment and interferes with light directly reflected from the surface. When the reflected and radiated light are in the same phase, constructive interference produces a sharp reflectance peak.

The reflectance peak can be designed to have very weak angular dependence. The peak wavelength can be tuned by varying the periodicity of the surface structure. The authors tested their concept with arrays of lithographically produced amorphous silicon rods on a glass substrate (see figure). These samples reflected a red color that was almost uniform over a wide range of viewing angles.

Because amorphous silicon absorbs in the smaller visible wavelength region, resonance was observed only for wavelengths >600 nm. The authors predict that other colors can be produced when other materials are used for the surface structures.

The authors also tested silicon rod arrays on an elastic polydimethylsiloxane substrate. This assembly process was more difficult; and the resulting samples had low macroscopic uniformity but acceptable nanoscopic accuracy. The substrate was stretched isotropically by fixing it to the surface of a balloon that was inflated gradually. Stretching the sample by 10% produced a 32-nm shift in the reflectance peak. (*ACS Photonics* DOI: 10.1021/ph500400w; Nancy McGuire)

http://www.acs.org/content/acs/en/noteworthy-chemistry/2015-archive/january-26.html#nc1

January 26, 2015

Blue laser light makes black "nanoflowers" glow red. The distinctive optical and magnetic properties of cobalt oxide (Co_3O_4) micro- and nanostructures make this material a strong contender in the development of photoelectronic devices. Most recent research on Co_3O_4, however, has focused on its applications as a catalyst and gas sensor and in lithium-ion batteries.

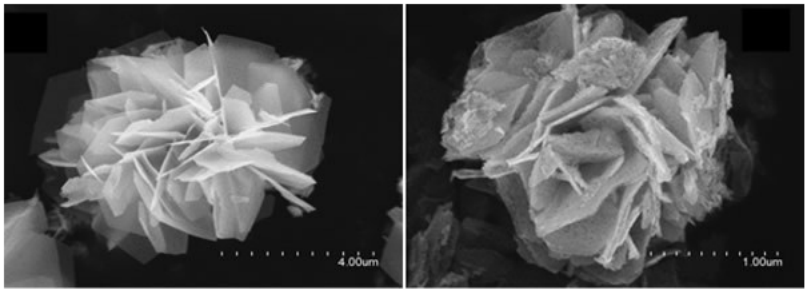

Co_3O_4 nanostructures composed of porous hexagonal plates

W. Wang* and J. Xu of Minzu University of China (Beijing) investigated the influence of the shape and size of Co_3O_4 nanostructures on the properties of the bulk material. These nanostructures include cubes, rods, sheets, and belts; but the current study focuses on flowerlike structures composed of thin plates (see figure).

The authors used a surfactant-free hydrothermal synthesis to produce hierarchically structured α-$Co(OH)_2$ assemblies that consist of green hexagonal plates a few tens of nanometers thick. The overall assemblies range from 2 to 10 μm along the diagonal direction. Annealing these structures in air converts them to black Co_3O_4 without changing the flowerlike morphology. High-resolution scanning electron microscope images of single hexagonal plates reveal that they are porous.

When they are excited by a helium–cadmium laser at 325 nm (visible blue light), these flowerlike assemblies have a broad photoluminescence band between 650 and 800 nm (visible red to near-infrared light), with a peak at 710 nm (1.75 eV). This result agrees well with the indirect optical band gap of 1.60 eV observed in Co_3O_4 thin films. The authors attribute the broad photoluminescence band to the wide range of sizes of the hexagonal plates. (*ACS Appl. Mater. Interfaces* DOI: 10.1021/am506414n; Nancy McGuire)

http://www.acs.org/content/acs/en/noteworthy-chemistry/2015-archive/january-19.html#nc5

January 19, 2015

This breathalyzer senses cancer. Effective cancer treatment relies on early detection and accurate assessment of treatment efficacy. One promising area of research is the identification of volatile organic compounds (VOCs) emitted by cancer cells. An ideal detector for these VOCs would detect low concentrations, respond rapidly to small changes in concentration, and provide a consistent output in response to a specific exposure.

H. Haick and coauthors at Technion—Israel Institute of Technology (Haifa); Max Planck Institute for the Science of Light (Erlangen, Germany); and the University of Latvia, Riga East University Hospital, and Digestive Diseases Center GASTRO (all in Riga, Latvia) developed an ultrasensitive VOC sensor and evaluated its effectiveness in a small pilot clinical study on exhaled breath samples. In a blind analysis, this sensor accurately discriminated between volatile compounds emitted by gastric cancer cells and control compounds, irrespective of such factors as tobacco consumption, Helicobacter pylori infection, and gender.

The sensor consists of an individual surface-modified silicon nanowire field-effect transistor (SiNW FET) with lock-and-key features that responds differently to various VOCs at the low-ppb level. The sensor also uses pattern-recognition methods for analyzing its response to complex mixtures. The authors tested various SiNW FET surface coatings for sensitivities to three compounds associated with gastric cancer cells and two compounds that exist in exhaled breath but do not correlate with the presence of cancer cells.

The sensors were evaluated with real breath samples from 30 cancer patients and 77 "healthy" volunteers, some of whom had dyspeptic symptoms but not cancer. Discriminant factor analysis was used to find the best possible separation between the cancer patients and the healthy volunteers.

Of the coatings tested, trichloro(phenethyl)silane produced the greatest sensitivity (5 ppb) toward the cancer-related VOCs and the greatest response difference between these compounds and the two non–cancer-related compounds. The training set for this coating showed 87% sensitivity, 81% specificity, and 83% accuracy. Plotting the blind samples onto this model achieved 71% sensitivity, 89% specificity, and 85% accuracy. The sensor distinguished little between smokers and nonsmokers and between patients with and without H. pylori infections.

This sensor had a sensitivity of 92% and a specificity of 67% for discriminating between advanced and early-stage gastric cancer. The authors suggest that the low specificity might be related to the small number of early-stage gastric cancer cases evaluated. (*Nano Lett.* DOI: 10.1021/nl504482t; Nancy McGuire)

http://www.acs.org/content/acs/en/noteworthy-chemistry/2015-archive/january-12.html#nc3

January 12, 2015

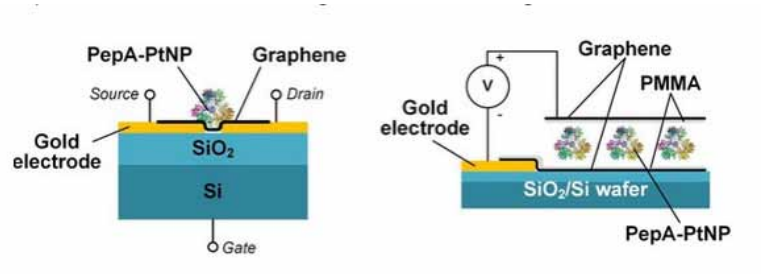

GFET (left) and biocapacitor (right)

Protein-shelled platinum and graphene form a nanocapacitor. Biosensors and embedded therapeutic devices would be improved if they contained flexible, biocompatible electronic components. These components may incorporate metallic or semiconducting nanoparticles that can be encased in hollow protein shells that control their size and stability, protect the nanoparticles, and reduce their toxicity. To date, there are few reports of electronic devices that incorporate protein-shelled nanoparticles; and little is known about their charge-transport properties.

T. Kim, K. K. Kim, and coauthors at Sungkyunkwan University and Medical School (Suwan), BIO-FD&C (Incheon), and Myongji University (Yongin, all in Korea) encapsulated platinum nanoparticles (PtNPs) inside PepA, a bacterial aminopeptidase molecule with a hollow center. They could vary the size of the PtNPs and thus tune the electronic properties of the protein-coated particles, by varying the ratio of precursor platinum ions to PepA.

The authors assembled a graphene-based field-effect transistor (GFET) with a SiO_2/Si substrate, gold electrodes, and an overlayer of graphene topped with PepA-PtNPs. The left side of the figure is a schematic diagram of the GFET.

Although proteins normally increase GFET conductivity, the encapsulated PtNPs reduced the conductivity of the GFET, possibly by acting as electron acceptors and hindering electron transfer between adjacent PepA molecules. Increasing the concentration of PepA-PtNPs reduced the GFET's conductivity further, possibly because surface adsorption of these particles enhances their ability to trap electrons from graphene.

Smaller PtNPs reduced conductivity more than larger ones, which confirms a previous observation that smaller NPs have greater charge-trapping capability. Thus, the size and concentration of NPs can be used to tune the conductivity of the GFET.

The authors also built a frequency-modulated capacitor by sandwiching an aqueous suspension of PepA-PtNPs between graphene layers coated with poly(methyl methacrylate) (PMMA; see schematic diagram at right in the figure). The specific capacitance decreased with increasing AC signal frequency and with the size of the PtNPs, possibly because of changes in the polarizability of the PepA-PtNP layer. (*ACS Nano* DOI: 10.1021/nn503178t; Nancy McGuire)

http://www.acs.org/content/acs/en/noteworthy-chemistry/2015-archive/january-5.html#nc6

January 5, 2015

Should you scrap your car or retrofit it? Vehicular transportation, a major contributor to fine particulate matter (PM) emissions, has increased rapidly worldwide. F. Yan, T. C. Bond*, and D. G. Streets at the University of Illinois at Urbana–Champaign, Argonne National Laboratory (IL), and the University of Chicago predict that if clean vehicle and clean fuel policies are not accelerated, more than 210,000 human lives and 25 million years of cumulative life could be lost to PM effects by 2030.

Current regulations for new-vehicle emissions have decreased emissions worldwide despite a growth in fuel use. The authors' previous studies showed that older vehicles and "superemitters" are now responsible for a large part of PM emissions. In this study, they used scenario analysis to examine two options—scrapping old vehicles or retrofitting them with emissions mitigation devices—to see how they would affect PM emissions.

Under the scrappage scenario, PM emissions worldwide would decrease rapidly as older vehicles are taken out of service, followed by a slow rise driven by increasing use of vehicles with poor or no emission controls in portions of Africa. As African countries adopt stricter emissions control standards, the emission levels begin to drop again. Under the most aggressive scenario, emissions would drop by 53–75% during the first 5–10 years and remain below the baseline (no-action scenario) until 2050.

Scrappage, in conjunction with the introduction of advanced emission control standards, is most effective in countries with a preponderance of old vehicles on the road. For regions without such standards and where retrofitting is impractical, scrappage with high compensation can help consumers purchase newer vehicles that can accommodate future retrofits as standards evolve.

For the retrofitting scenario, the largest emission reductions (16–31% below the baseline) occur 25–35 years after the program begins, following a lag time in the adoption of advanced technologies and regulations in low-income regions. The retrofits that the authors studied can be used only on diesel vehicles with relatively new engines, which are not widely available in poorer countries. Retrofitting is preferable for high-income regions, where there are fewer old vehicles on the road and high-quality fuels are easily obtainable. Even though the emission reductions by scrappage and retrofitting are comparable in these regions, retrofitting is likely to be less expensive for the consumer. (*Environ. Sci. Technol.* DOI: 10.1021/es503197f; Nancy McGuire)